Proceedings of the 3rd International Conference on Fluid Flow and Thermal Science (ICFFTS'22)
Virtual Conference - October 27 - 29, 2022
Paper No. 117
DOI: 10.11159/icffts22.117

Investigation of Nano Thin Film Evaporation on Hot Spot with Nanopillar Array Based on Molecular Dynamics Simulation

Xianghui Huang, Runkeng Liu, Zhenyu Liu*
School of Mechanical Engineering, Shanghai Jiao Tong University
800 Dong Chuan Road, Shanghai, China
hxh1998@sjtu.edu.cn; 1073407134@sjtu.edu.cn; zhenyu.liu@sjtu.edu.cn

Abstract - In the nano-thin film evaporation process, the hot spots may experience the local dry out phenomenon, which shows a low heat transfer performance. In present study, one stable evaporation of nano-thin water film on the substrate with different nanopillar structures was investigated using the non-equilibrium molecular dynamics (MD) approach. It shows that the nanopillar array can replenish the hot spot by attracting the surrounding water out of the overheated region, both the stability and performance of evaporative heat transfer can be improved. The effect of the number of nanopillars on the evaporation process was studied. The prediction indicates that evaporation rate is important to the replenishment. With the increasing amount of nanopillars, both the evaporative heat transfer and liquid replenishment ability are improved accordingly. The results in present work can contribute to the thermal control of the hot spot in the embedded liquid cooling technique for the high-power electronic chip.

***Keywords*:** Evaporation, Hot spot, Nanopillar array, nano-thin water film, MD

1. Introduction

The liquid-gas phase change heat transfer has been extensively investigated on atomic scale in past years [1-5]. Compared to the boiling heat transfer, the evaporative one is an effective approach to the cooling technology as it has high and stable heat dissipation capability [6, 7]. For now, the nanoscale evaporation began to be utilized in the innovative devices, such as electronic chip cooling [7, 8], heat pipe [9], solar vapor generation [10], water desalination [11], etc. However, in the high-power electronic chip, the local dry out may occur on the hot spots (overheated regions), resulting in a deterioration of heat transfer. To overcome this disadvantage, it is necessary to find the method to maintain the high-efficient and stable evaporative heat transfer for the nano-thin liquid film.

Previous works have been performed on the evaporative heat transfer of thin film on uniform-temperature substrates [12-14], which indicate that the evaporation process can be enhanced by adding nanostructures onto the substrate. Several experimental results showed that micropillar array or nanowire array has a superior wicking ability, which can achieve a liquid replenishment and maintain a stable evaporative heat transfer of liquid film. Adera et al. [15] carried out the experimental work to study the thin liquid film evaporation on the silicon micropillar wicks without the nucleate boiling, and a semi-analytical model was established in the determination of the capillary-limited dry out heat flux and the related wall temperature. Ravi et al. [16] experimentally investigated the wicking ability and dry out of different micropillar arrays, and proposed one model to predict the mass transport ability with the micropillar arrays. Wen et al. [17] constructed a two-level hierarchical substrate with patterned Cu nanowire arrays, for which the shorter nanowires surrounded by the longer ones. It shows that the modified substrate can be rewetted due to the capillary effect. However, based on the review work of previous studies, there are few reports on the prevention of the local dry out on the hot spots. Therefore, the need to reveal the related evaporation characteristic and propose a solution to achieve a stable performance is urgent.

In present study, we constructed one substrate with nanopillar array on the hot spot, and the non-equilibrium MD simulation was utilized to predict the steady evaporation of nano-thin water film on it. The water molecular motion trajectories, evaporation rate of the water film and number of migrating water molecules in different regions on the substrate were recorded over time in the MD simulation. The effect of amount of nanopillars on the evaporation of nano-thin water film and the liquid replenishment of the hot spot performances was discussed based on the obtained data.

2. Simulation method

The MD models are shown in Fig. 1, three substrates with different nanopillar numbers (N=5, N=6 and N=7) on the pink circular regions (radius of 2.5 nm) are constructed, the pink circular region presents the hot spot (overheated region), and the nano-thin water film is transparently shown for a better understanding. The simulation box in present model is a cuboid one with a size of 10 nm × 10 nm × 25 nm. The periodic boundary conditions are adopted in all directions. In order to obtain how many water molecules are evaporated, one cooling plate is set on the top. All nanopillars on the hot spots for different simulation cases have the same size (5 nm high and 1.1 nm diameter). The first layer of cooling plate and the last layer of substrate are fixed to avoid the loss of the atoms, and two layers close to them are arranged as the phantom ones (heat sources). The rest regions of the solid part are considered as the conduction layers in numerical simulation.

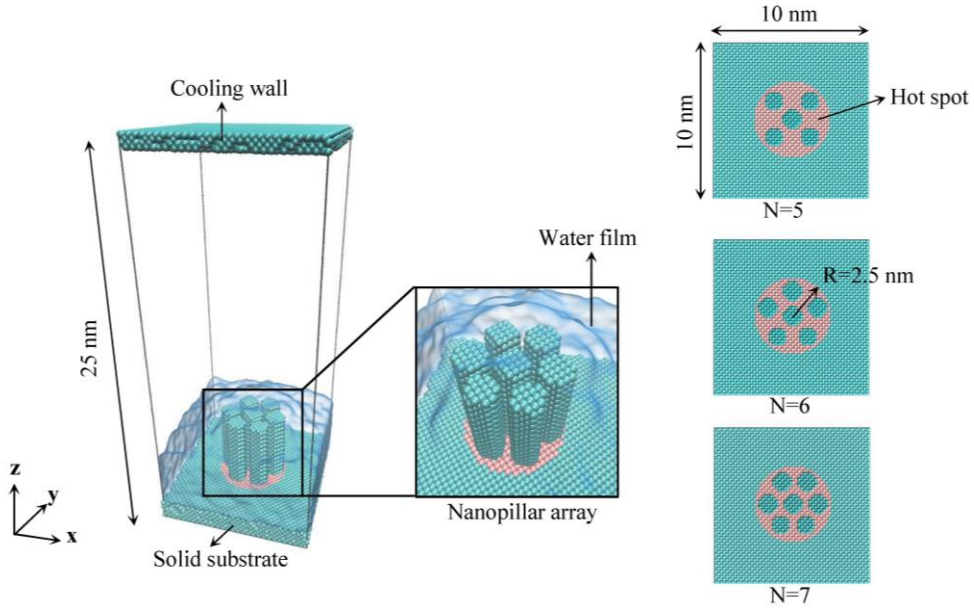

Fig. 1: Schematic illustration of simulation system.

In the established model, both cooling plate and solid substrate are copper ones, which are FCC structured with a lattice constant of 3.61 Å. The TIP3P water molecules model is adopted, which is widely used in the previous modeling, and the water molecules numbers of the water film for different cases are kept the same (around 13790) before starting the simulation. The standard 12/6 L-J potential is utilized to predict the short-range van der Waals interaction and Coulombic potential is used in the calculation of the long-range electrostatic interaction. The potential function can be expressed as follows:

$$E = 4\varepsilon\left[\left(\frac{\sigma}{r}\right)^{12} - \left(\frac{\sigma}{r}\right)^{6}\right] + \frac{Cq_iq_j}{r} \tag{1}$$

where ε and σ are the energy and length parameters, r is the distance between two molecules/atoms, C is an energy-conversion constant, q_i and q_j are the charges on the two atoms. The van der Waals interaction and electrostatic interaction will be neglected as the distance between two atoms is larger than is 1.0 nm and 1.2 nm, respectively. The detailed information is shown in Table 1. The Lorentz-Berthelot combination rule is used in the selection of the pairwise coefficients for the interactions between two different atoms.

Table 1: Values of potential parameters.

Atom	ε (eV)	σ (Å)	q (e)
Cu	0.4096	2.340	0
O	0.0067	3.166	-0.83
H	0	0	0.415

One artificial spring force is applied to all Cu atoms and bind them near their initial position. The potential energy of the spring force is calculated with Hooke's law:

$$\emptyset_{Cu} = \frac{1}{2}\sum_i k(r_i - r_i^0)^2 \tag{2}$$

in which $k = E \cdot d$, E (120 GPa) is the Young's Modules of Cu, d is the lattice constant of Cu, r_i is the ith atom position and r_i^0 is its equilibrium position.

All the simulations are performed with LAMMPS [18]. The velocity-Verlet integration method is used with a time step of 5.0 fs. The long-range Coulomb interactions are calculated by the particle-particle particle-mesh method under a relative accuracy of 10^{-4}. All calculation processes can be categorized by three steps: (1) minimization, (2) equilibrium (constant temperature and relaxation) and (3) evaporation. In step (1), the conjugate gradient (CG) algorithm is used to constantly adjust atom coordinates for energy minimization of the system until the energy tolerance is smaller than 10^{-8} or force tolerance smaller than 10^{-10}. In step (2), firstly, the Langevin thermostat is applied to all atoms to increase the system temperature to 300 K within 1ns. Then, the Cu atom temperature maintains at 300 K by the Langevin thermostat within 1ns, while the water molecules are simulated with the NVE ensemble at the same time to make the system is equilibrated to a stable state. In step (3), to predict the evaporation on the hot spot, the temperature of the circular region (600 K) is higher than the surrounding one (360 K), while the cooling plate is set at 290 K to condense evaporated water molecules. All the temperatures are instantly increased or decreased from 300 K to the specified temperature with the Langevin thermostat as the evaporation process starts. Only the data of evaporation step is recorded and utilized for the following analysis.

3. Simulation Method

The nano-thin water film evaporation on hot spot with nanopillar array is simulated with the non-equilibrium MD method, and the effect of the amount of nanopillars (N=5, N=6 and N=7) on the evaporation performance is investigated accordingly. By tracking the motion trajectories of water molecules, the change of the water film thickness with time can be obtained. Fig. 2 shows the snapshots of water film during the evaporation process. It can be found that the water film thickness decreases with time, which decreases more rapidly as the number of nanopillars increases. Fig. 3 shows the variation of evaporated water molecule number with time. The results show that the evaporation rate increases with increasing nanopillar number, which indicates the evaporative heat transfer is improved accordingly. The addition of nanopillars enlarges the heat transfer area, and more heat in hot spot region can be dissipated by the water undergoing the evaporation process.

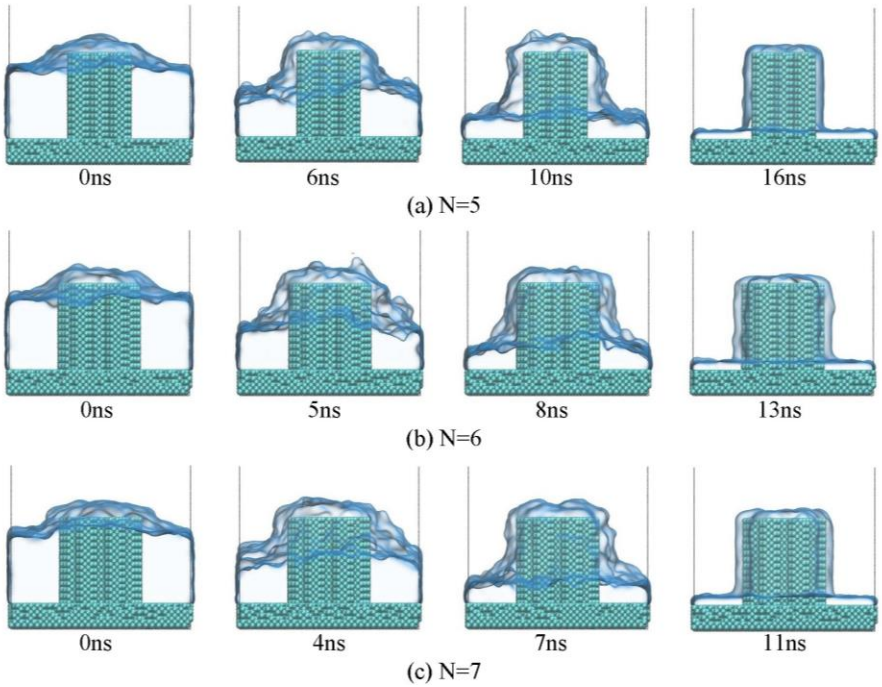

Fig. 2: Snapshots of evaporation processes for surfaces with different number nanopillars on hot spot.

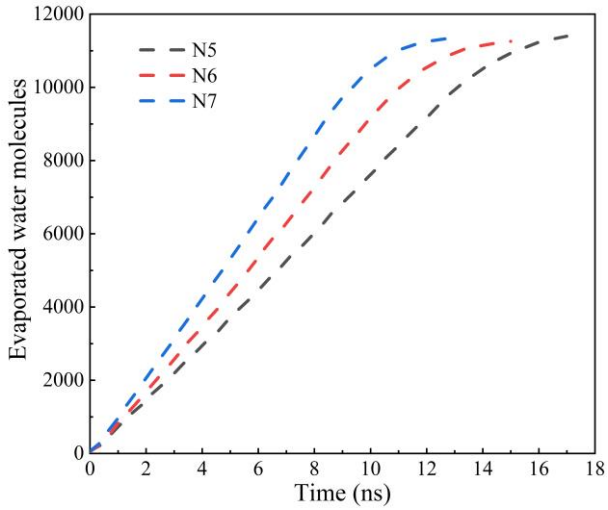

Fig. 3: Number of evaporated water molecules.

It should be noted that despite the temperature of the hot spot region is much higher than that of other region, there exists no nucleated boiling or local dry out in the simulation. The nanopillar array is always covered by water film, undergoing a steady evaporation process, which indicates that the surrounding liquid molecules should constantly migrate to the hot spot to replenish the evaporated ones. Therefore, to prove the liquid replenishment phenomenon occurs, the water film can be divided into nanopillar region and flat region. The first region is a cylindrical one with a radius of 3 nm, whose center and radius are selected based on the thickness of water molecules wrapped around the nanopillar array, and the rest of the water film is a flat region. Then the migrating water molecule numbers between two regions with time can be calculated, which is show in Fig. 4. For this purpose, the coordination number (CN) and

coordinates of each oxygen atom are recorded first, and the liquid-vapor interface can be determined by CN. When the CN is continuously greater than the critical coordination number (CN = 6) and the z-coordinate is continuously less than 8 nm, the water molecule is considered as still in liquid state. Therefore, liquid water molecules located in the nanopillar region and flat region can be screened out. The changes of water molecule number and position in the liquid film were counted. And the variation of the migrating water molecule number between two regions and the evaporation flux over time were obtained, as shown in Figs. 4 and 5, respectively.

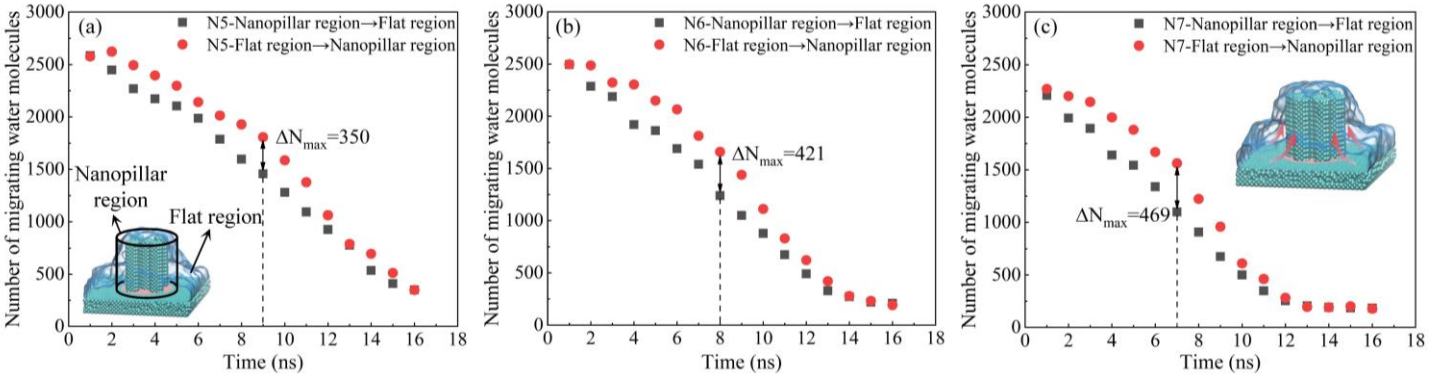

Fig. 4: Number of migrating water molecules between two regions: (a) N=5; (b) N=6; (c) N=7.

Due to the thermal motion of the water molecules, their migration occurs between two regions. At the start of evaporation, the difference in the water molecules migrating between two regions is not obvious. As evaporation goes on, the water molecules migrating from flat region to nanopillar one is significantly greater than that in the opposite direction, and its difference can be considered as the liquid replenishment.

$$\Delta N = N_{FN} - N_{NF} \tag{3}$$

where N_{FN} is the water molecule number migrating from flat region to nanopillar one, N_{NF} is the water molecule number migrating from nanopillar region to flat one.

As the ΔN is positive, it means that the surrounding liquid water constantly moves into the nanopillar region to maintain it is always wetted. This phenomenon can be discussed based on the atomic interaction. Firstly, the interaction between Cu atom and oxygen atom is stronger than that between oxygen atoms, which indicates water molecules are more likely to be attracted by Cu atoms. For another, as a water molecule is closer to the nanopillar array than to the surface of the substrate, it is more likely to be attracted to the nanopillar. Therefore, as part of the water molecules in the nanopillar region evaporate, the surrounding liquid water will move into nanopillar array to achieve continuous replenishment and realize a stable evaporation. As the water film thickness decreases to a certain extent, the attraction between Cu atoms in substrate and water molecules in flat region gradually become stronger, and the water molecules that can overcome this attraction decreases, that is why the liquid replenishment gradually weakens as the evaporation progress reaches a certain point.

At the end of evaporation, the liquid replenishment stops, and there exists one non-evaporated layer near the solid surface caused by the strong solid-fluid interaction, which has been reported in the previous studies [19, 20]. In addition, as the contact area between the two regions decreases with the evaporation process, the water molecules migrating between the two regions decreases with time. It can be found that the maximum liquid replenishment increases with the increasing nanopillars, and the moment of the maximum value appearing is also earlier, which indicates that more nanopillars can improve the capability of liquid replenishment.

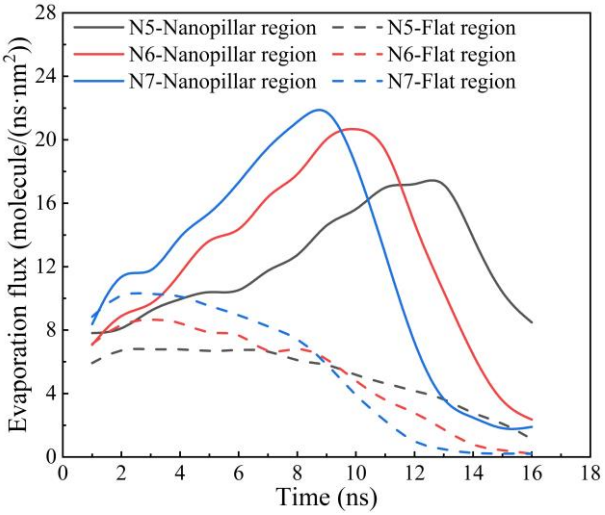

Fig. 5: Variation of evaporation flux during evaporation processes.

Figure 5 shows the change of evaporation flux with time in different cases. It indicates that the evaporation flux in the nanopillar region increases first and then decreases rapidly. By comparing the results of different nanopillars, it is found that with the increasing nanopillar number, the evaporation flux of nanopillar region increases faster in the early stage and decreases faster when the surface is nearly dry out. The evaporation flux increases faster because the amount of liquid replenishment is sufficient in the early stage and the heat transfer area is enlarged with more nanopillars. The amount of liquid replenishment also decreases faster with more nanopillars when the surface is nearly dry out. When the liquid replenishment cannot be timely, the evaporation flux decreases faster with the increasing nanopillar number. Moreover, the evaporation flux of hot spot is normally larger than that of the flat one. The higher evaporation flux contributes to the heat removal of hot spot surface, while the different evaporation flux between two regions is one important reason for the liquid replenishment. Through the comparison, the maximum evaporation flux of hot spot increases with the increasing nanopillar number and it appears earlier, which is similar to trend of the liquid replenishment. It means evaporation rate is an important factor affecting the liquid replenishment ability.

4. Conclusion

In this work, the nano-thin water film evaporation on hot spot with nanopillar structure is studied with the non-equilibrium MD simulation. It is found that the nanopillar array can attract the surrounding liquid water to replenish the hot spot, both stability and performance of evaporative heat transfer are improved. Moreover, the influences of the nanopillar number on the evaporation process and liquid replenishment are compared based on the obtained data. It shows that evaporation rate is an important factor affecting the liquid replenishment. With the increasing nanopillars, the evaporation efficiency and liquid replenishment ability are both improved, which can maintain one stable evaporation. The conclusions in present work can contribute to the thermal control of the hot spot in the embedded liquid cooling technique for the high-power electronic chip.

Acknowledgements

This work was supported by the National Natural Science Foundation of China through grant no. 51676124 and Shanghai International Science and Technology Cooperation Project through grant no. 18160743900.

References

[1] X. Yin, C. Hu, M. Bai, and J. Lv, "An investigation on the heat transfer characteristics of nanofluids in flow boiling by molecular dynamics simulations," *Int. J. Heat Mass Tran.,* vol. 162, p. 120338, 2020.

[2] H. Liu, X. Qin, S. Ahmad, Q. Tong, and J. Zhao, "Molecular dynamics study about the effects of random surface roughness on nanoscale boiling process," *Int. J. Heat Mass Tran.,* vol. 145, p. 118799, 2019.

[3] R. Liu and Z. Liu, "Study of boiling heat transfer on concave hemispherical nanostructure surface with MD simulation," *Int. J. Heat Mass Tran.,* vol. 143, p. 118534, 2019.

[4] R. Liu and Z. Liu, "Rapid thermal transport at rough solid-fluid interface: Evaporation and explosive boiling on concave nanostructure," *Int. J. Heat Mass Tran.,* vol. 154, p. 119676, 2020.

[5] Z. Liu, R. Liu, P. Li, A. Xu, and Z. Liu, "Study of Boiling Heat Transfer on Heterogeneous Wetting Surface With MD Simulation," in *ASME 2021 Heat Transfer Summer Conference collocated with the ASME 2021 15th International Conference on Energy Sustainability*, 2021, vol. ASME 2021 Heat Transfer Summer Conference, p. V001T08A005.

[6] B. V. Deryagin, S. V. Nerpin, and N. V. Churaev, "To the theory of liquid evaporation from capillaries," *Kolloidn. Zh.,* vol. 26, pp. 301-307, 1964.

[7] R. Liu and Z. Liu, "Enhanced Evaporation of Ultrathin Water Films on Silicon-Terminated Si3N4 Nanopore Membranes," *Langmuir,* vol. 37, no. 33, pp. 10046-10051, 2021.

[8] R. Liu and Z. Liu, "Self-pumping ultra-thin film evaporation on CNT-embedded silicon nitride nanopore membrane," *Nano Res.,* vol. 15, no. 3, pp. 1725-1729, 2022.

[9] E. Norouzi, C. Park, and G. Hwang, "Nanoscale heat pipe using surface-diffusion-driven condensate return," *Int. J. Heat Mass Tran.,* vol. 130, pp. 1238-1248, 2019.

[10] P. Tao, G. Ni, C. Song, W. Shang, J. Wu, J. Zhu, G. Chen, and T. Deng, "Solar-driven interfacial evaporation," *Nature Energy,* vol. 3, no. 12, pp. 1031-1041, 2018.

[11] S. P. Surwade, S. N. Smirnov, I. V. Vlassiouk, R. R. Unocic, G. M. Veith, S. Dai, and S. M. Mahurin, "Water desalination using nanoporous single-layer graphene," *Nat. Nanotechnol.,* vol. 10, no. 5, pp. 459-464, 2015.

[12] Q. Cao, W. Shao, X. Ren, X. Ma, K. Shao, Z. Cui, and Y. Liu, "Molecular dynamics simulations of the liquid film evaporation heat transfer on different wettability hybrid surfaces at the nanoscale," *J. Mol. Liq.,* vol. 314, p. 113610, 2020.

[13] S. Cai, Q. Li, W. Li, L. Zhang, and X. Liu, "Effects of mole fraction and surface wettability on evaporation of Ar/Kr mixtures: A molecular dynamics study," *J. Mol. Liq.,* vol. 319, p. 114189, 2020.

[14] S. Cai, C. Wu, X. Li, and Q. Li, "Effects of lubricant on evaporation and boiling processes of R1234ze(E): A molecular dynamics study," *Appl. Therm. Eng.,* vol. 193, p. 117009, 2021.

[15] S. Adera, D. Antao, R. Raj, and E. N. Wang, "Design of micropillar wicks for thin-film evaporation," *Int. J. Heat Mass Tran.,* vol. 101, pp. 280-294, 2016.

[16] S. Ravi, D. Horner, and S. Moghaddam, "Monoporous micropillar wick structures, I-Mass transport characteristics," *Appl. Therm. Eng.,* vol. 73, no. 1, pp. 1371-1377, 2014.

[17] R. Wen, Q. Li, W. Wang, B. Latour, C. H. Li, C. Li, Y.-C. Lee, and R. Yang, "Enhanced bubble nucleation and liquid rewetting for highly efficient boiling heat transfer on two-level hierarchical surfaces with patterned copper nanowire arrays," *Nano Energy,* vol. 38, pp. 59-65, 2017.

[18] S. Plimpton, "Fast Parallel Algorithms for Short-Range Molecular Dynamics," *J. Comput. Phys.,* vol. 117, no. 1, pp. 1-19, 1995.

[19] X. Deng, Y. Xiao, Q. Li, C. He, and S. Wang, "Evaporation of R1234yf, R1234ze(E) and R1234ze(Z) on Cu surface: A molecular dynamics study," *J. Mol. Liq.,* vol. 344, p. 117844, 2021.

[20] B. Peng, W. He, X. Hao, Y. Chen, and Y. Liu, "Interfacial thermal conductance and thermal accommodation coefficient of evaporating thin liquid films: A molecular dynamics study," *Comp. Mater. Sci.*, vol. 87, pp. 260-266, 2014.